Plasmonic Metamaterials: Physical Background and Some Technological Applications

Benjamin G. Schmidt

A Senior Thesis submitted in partial fulfillment
of the requirements for graduation
in the Honors Program
Liberty University
Spring 2019

Acceptance of Senior Honors Thesis

This Senior Honors Thesis is accepted in partial fulfillment of the requirements for graduation from the Honors Program of Liberty University.

_____

Carl Pettiford, Ph.D.
Thesis Chair

_____

Hector Medina, Ph.D.
Committee Member

_____

Amy Drambi, M.S.
Committee Member

_____

Mark Ray Schmidt, Ph.D.
Assistant Honors Director

_____

Date

Abstract

New technological frontiers appear every year, and few are as intriguing as the field of plasmonic metamaterials (PMMs). These uniquely designed materials use coherent electron oscillations to accomplish an astonishing array of tasks, and they present diverse opportunities in many scientific fields.

This paper consists of an explanation of the scientific background of PMMs and some technological applications of these fascinating materials. The physics section addresses the foundational concepts necessary to understand the operation of PMMs, while the technology section addresses various applications, like precise biological and chemical sensors, cloaking devices for several frequency ranges, nanoscale photovoltaics, experimental optical computing components, and superlenses that can surpass the diffraction limit of conventional optics.

Plasmonic Metamaterials: Physics and Technological Applications

Introduction: What is a plasmonic metamaterial?

Centuries of scientific and technological progress has led to technological advances that previous generations could not imagine, and with each passing year, the many different fields of science and engineering gradually converge to develop multidisciplinary technology with many applications. One of the most interesting recent examples of this innovative convergence is the field of plasmonic metamaterials.

A plasmonic metamaterial (PMM) is an artificially designed material that uses quasiparticles called surface plasmons to demonstrate unique properties and capabilities not found in natural materials. In order to more fully understand PMMs and their applications, it is first necessary to address several underlying concepts: the nature of subatomic particles and quasiparticles, the behavior of electrons in different materials (specifically band theory), plasmons, surface plasmon polaritons, and metamaterials.

Fermions, Bosons and the Standard Model

In particle physics, the Standard Model is a theory that summarizes the properties of three of the four known fundamental forces: the weak, strong, and electromagnetic forces. The model also classifies all elementary particles into groups and subgroups (Mann, 2010, pp. 9-18). This model represents the sum of experiments and accompanying theories of many scientists around the world over several decades. It is thought to be internally consistent, and no known experiments have disproven (Mann, 2010, p. 19). However, the Standard Model does not sufficiently explain several important phenomena. It does not fully incorporate gravity as described by general relativity, primarily because gravity has not yet been fully reconciled with quantum

mechanics. It also does not adequately explain the presence or properties of dark matter and dark energy (Carroll, 2007, p. 31), the baryon asymmetry problem[1], or the oscillations of neutrinos between different lepton family numbers (Barger, Marfatia & Whisnant, 2012, pp. 99-115).

The Standard Model separates all elementary particles (and some quasiparticles, as will be seen later) into one of two primary groups: fermions, which adhere to the Fermi-Dirac statistics, and bosons, which adhere to the Bose-Einstein statistics. Fermions, in a general sense, can be thought of as the particles that matter is "made of," while bosons are the "glue" holding it together (Carroll, 2013). All fermions obey the Pauli exclusion principle, which states that no two fermions can occupy the same energy state (or quantum state) if they are in the same system. Bosons are not held to the same restriction.

Fermions have a half-integer spin number, while bosons have integer spin numbers[2]. This forms the basis for the spin-statistics theory in relativistic quantum field theory, which, among other things, states that integer-spin particles cannot be fermions, and half-integer-spin particles cannot be bosons (Sakurai, p. 363). One of the most distinctive differences between fermions and bosons occurs at extremely low temperatures; at such temperatures, systems comprised of bosons will condense into the same ground state, known as a Bose-Einstein condensate, while fermions normally do not demonstrate the same property[3].

---

[1] I.e. the imbalance of baryonic matter and antimatter in the observed universe.
[2] The spin number is one of the four quantum numbers that describe the properties of particles.
[3] Under certain conditions, including a lower temperature than that required for a Bose-Einstein condensate, fermions can combine into bosonic compound particles known as Cooper pairs, which can form Bose-Einstein condensates (Regal, Greiner & Jin, 2004).

Band Theory

In solid-state physics, the *electronic band structure* defines the energy ranges that electrons can and cannot occupy, called *energy bands* and *band gaps* respectively. The body of knowledge concerning electronic band structures is known as *band theory*, and its conclusions are derived by observing the quantum mechanical wave functions of the electrons in atomic or molecular lattices[4]. Band theory has helped explain many important physical phenomena, like optical absorption, electrical resistivity, and solid-state physics.

In band theory, the valence band and conduction band are those bands which are closest to a material's Fermi level[5], and their relative energy distance determines the conductivity of the material. In non-conductors, the valence band is below the Fermi level and the conduction band is above. The valence band is the highest range of electron energy states occupiable at absolute zero, while the conduction band is the lowest vacant electron energy band. As materials become more conductive, the band gap between the valence and conduction bands shrinks until the two bands overlap, and the overlapping bands take on the properties of both valence and conduction bands, as shown in Figure 1.

Electrons and the Free Electron Gas

In conductive materials, like metals, electrons are not bound to specific atoms as they are in insulative materials. Instead, they are shared amongst all the atoms in the

---

[4] A *wave function* describes the quantum state of a given quantum system.

[5] The *Fermi level* is a measure of electrochemical potential that represents the thermodynamic work required to add an electron to the system, and is dependent on several factors, namely the temperature of the system, and the number and effective masses of electrons and holes. Note that the Fermi level should not be confused with the Fermi *energy*, which is the energy differences between the highest and lowest energy states in a system at absolute zero.

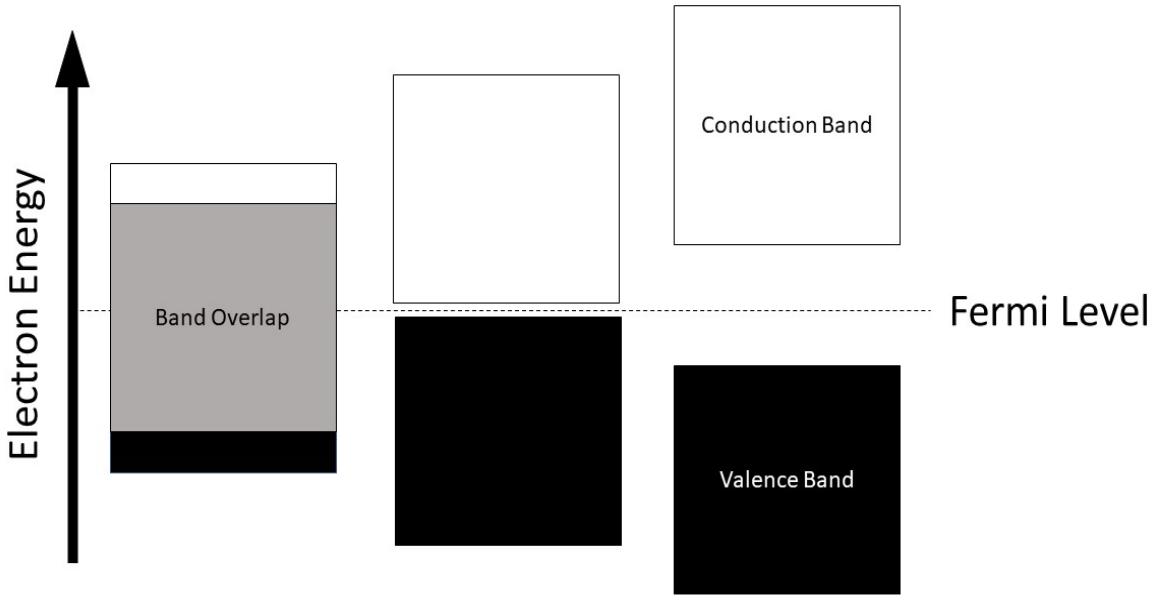

Figure 1: Valence and conduction bands for metals, semiconductors, and insulators.

material and are free to move around the atomic array structure in response to external stimuli; this group of electrons is referred to as the free electron sea or the free electron gas. This sea of electrons behaves like a plasma in some regards. Because of this, even though metals are not truly plasma, they are often modeled as such when considering certain properties, especially optical ones, as Figure 2 demonstrates.

Electrons are fermions, so they must adhere to the Pauli exclusion principle, namely that no two electrons bound to an atom can have the same values of the four quantum numbers[6]. In an electron sea, like the one described above, the same rule applies, because all the atoms exist in the same system; however, the energy difference between the conduction and valence band in a conductor is substantially smaller than in

[6] Namely the principal number *n,* the angular momentum number *l*, the magnetic number m_l, and the spin number m_s.

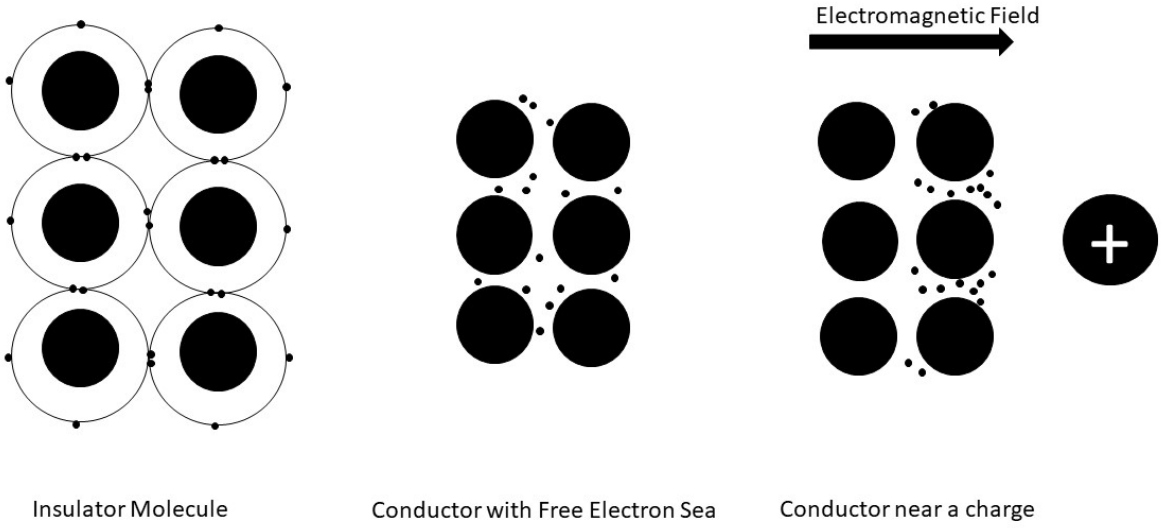

Figure 2: Electrons in insulators and conductors.

in an insulator and will usually overlap, as seen in Figure 1. Also, the number of molecular orbitals in semiconductors and conductors is so high that they essentially form a continuous energy band structure, which has an influence on many of the properties of these materials. The average number of fermions in a single-particle state *i* in a given system is given by the sigmoid (S-shaped) Fermi-Dirac distribution:

$$\bar{n}_i = \frac{1}{e^{(\epsilon_i - \mu)/k_B T} + 1} \qquad \text{(Eq. 1)}$$

where n_i is the number of fermions in the energy state, ϵ_i is the energy of the single-particle state *i,* k_B is Boltzmann's constant, T is the absolute temperature, and μ is the total chemical potential. If one considers the electrons within a conductor as members

of a quantum system for which the potential for the system is established by the stationary positive ion cores (in this case, the individual metal atoms), the quantum system will respond to external stimuli as a system, rather than acting as individual particles (Hornyak, Dutta, Tibbals, & Rao, 2008, pp. 275-276).

Plasmons

A plasmon is a quasiparticle consisting of the collective oscillations of an electron system. In physics, a quantum is the minimum possible amount of a physical entity involved in an interaction. If a property or entity can only exist in specific, discrete values, the property or entity is said to be *quantized*. Thus, a plasmon is a quantum of plasma oscillation in much the same way that a photon is a quantum of light oscillation, a phonon is a quantum of vibrational energy, or the energy of an electron is quantized.

Much like light, plasmons can behave as both a wave and a particle. When viewed as a wave, plasma oscillations are known as Langmuir waves, after Irving Langmuir, an American chemist and physicist. Unlike electrons, plasmons are bosons, so they adhere to the Bose-Einstein statistics and are not bound by the Pauli exclusion principle.

Surface plasmons. When light strikes the surface of a metal, the oscillating electric portion of the light wave interacts with the electrons that make up the free electron gas, causing these electrons to oscillate relative to the strength of the electric field. This packet of oscillating electrons is confined to the surface of the material and is known as a *surface plasmon* or SP. When the SP oscillates, the motion of its constituent electrons generates an opposing electric field that is slightly out of phase with the incident light wave. This, incidentally, is the reason that metals are opaque and appear shiny: the light wave is collected and then reflected toward the source.

Formation of SPs is not limited to light propagating from air to a metal; at any interface between two materials where the sign of the real part of the permittivity[7] changes sign over the interface, a surface plasmon can form. The material with positive real permittivity is known as the dielectric material, and that with the negative is known as the plasmonic material. The excitation of the system due to the incident light is either called a *localized surface plasmon* or a *surface plasmon polariton*.

Localized surface plasmons. In metallic nanoparticles that are of comparable size to the wavelength of incident light or smaller, a localized surface plasmon, or LSP, will form. When these conditions are met, the electric field of the incident light wave induces an electric dipole in the metallic nanoparticle (Ashby, Ferreira & Schodek, 2009, pp. 231-232). LSPs have two properties of interest: the electric fields near the surface of the particle are amplified significantly due to the concentrated response of the plasmon near the particle, and the particle's maximum optical absorption corresponds to the plasmon's resonant frequency (Dragoman & Dragoman, 2009, p. 325). There are several interesting applications for LSPs, but they will not be a primary focus of this thesis.

Surface plasmon polaritons. A surface plasmon polariton, or SPP, is an electromagnetic oscillation that travels parallel to an interface between two materials for which the sign of the permittivity changes across the interface, as explained above. The term surface plasmon polariton is derived from the wave's origins in both coherent charge motion in the metal (surface plasmon) and electromagnetic waves propagating parallel to the interface (polariton). Essentially, SPPs are "light waves trapped on the

[7] Considering permittivity as a complex number, as will be explained in greater detail below.

interface between one material and another, as a result of interactions between the incident wave and existing free electrons" (Ashby et al., 2009, p. 231). SPPs are evanescent, and their propagation along the surface can be guided, similarly to how light can be guided through an optical fiber or waveguide. They will continue to propagate along the interface until their energy is absorbed into the metal or it scatters away from the interface. An SPP has a much shorter wavelength than the incident light that initiates it; as a result, it also has higher local field strength and tighter quantum confinement[8]. These are the primary properties from which most SPP applications are derived.

SPP excitation

SPPs can be excited by several methods; this excitation is also sometimes referred to as a coupling of the SP with the incident wave. The first, and most straightforward, is by firing a beam of electrons into the bulk metal. The component of scattered oscillations due to the excitation from the beam that is parallel to the interface creates an SPP (Ashby et al., 2009, p. 231).

Another method involves excitation via photons. This is more difficult, though: photons and plasmons have different dispersion relations, which describe the relationship between their respective wavelengths and frequencies. The wave vector of a surface plasmon is given by:

[8] Quantum confinement refers to the increasingly discretized occupiable energy bands of a particle as it decreases in size.

$$k_{plasmon} = \frac{\omega}{c}\sqrt{\left(\frac{\varepsilon_M \varepsilon_D}{\varepsilon_D + \varepsilon_M}\right)} \quad \text{(Eq. 2)}$$

where k_x is the wave vector of the plasmon, ω is the angular frequency of the wave, c is the speed of light in vacuum, ε_M is the permittivity of the metallic medium, and ε_D is the permittivity of the dielectric medium (Kan & Liu, 2014; Aust, Sawodny, Ito & Knoll, 1994). Conversely, the wave vector for a photon is simply:

$$k_{photon} = \frac{\omega}{c} \quad \text{(Eq. 3)}$$

where ω and c represent the same factors as before. As can readily be observed, the wave vector of a photon is not dependent on the permittivities of either media.

A plasmon oscillating at a given frequency will generally have a greater momentum than an electron at the same frequency, due to their different dispersion relations (Figure 3). Plasmons in the bulk of the metal will demonstrate the strongest oscillation response at the bulk plasma resonant frequency ω_p, which varies for different materials.

At low frequencies, the parallel propagation of the SPP results in a dispersion relation like that of a photon propagating in free-space; this form of the SPP is known as

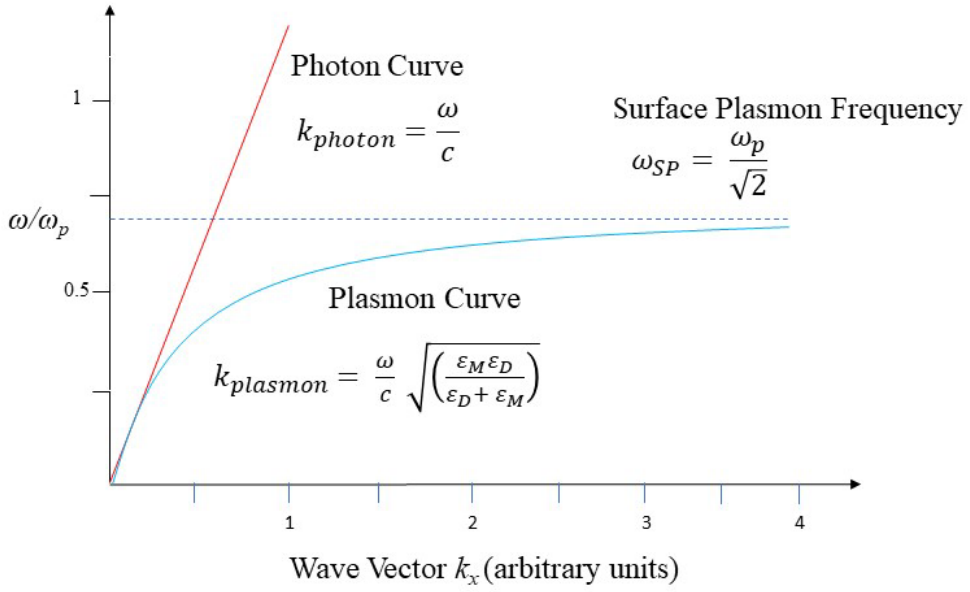

Figure 3: Photonic and plasmonic dispersion relations, with air as a dielectric and silver as a conductor

a Sommerfeld-Zenneck wave, demonstrated by the plasmon curve approaching the photon curve in Figure 3. At higher frequencies, the dispersion relation deviates from the photonic curve and approaches an asymptotic limit known as the surface plasma frequency, ω_{SP}. The asymptote exists because an SPP has a shorter wavelength than light of the same frequency, and experiences evanescent losses as frequency increases because the absorption rate of the metal is high at optical frequencies. Because momentum and energy must be conserved, a photon must acquire additional energy to reach the momentum required to pair with a surface plasmon.

This momentum mismatch means that photons traveling through free space, or any dielectric that does not meet specific conditions, cannot couple to a surface plasmon on a metallic surface, and for the same reason, an SPP cannot emit energy into a dielectric as a photon.

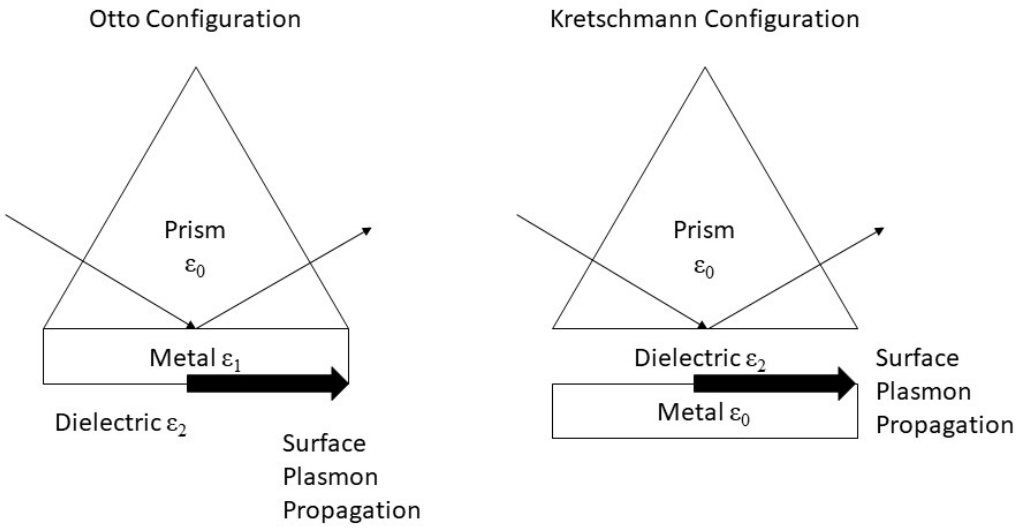

Figure 4: Otto and Kretschmann Lens Configurations.

This momentum inequality can be overcome by using a coupling medium, like a prism, grating, or a deformity on an otherwise planar surface to match the wave vector of the photon to that of the SPP (which also matches their momenta). There are two options for prism configuration. The first is the Kretschmann configuration, in which a prism is put in direct contact with the metal surface. This creates an SPP on the opposite side of the metal from the incident light, like the left part of Figure 4 (Kretschmann & Raether, 1968). The second is the Otto configuration, which positions the prism a small distance away from the metal surface, utilizing the air gap as a dielectric. In this configuration, the SPP forms on the side of the metal closer to the incident wave, as seen on the right of Figure 4 (Otto, 1968).

A less common coupling method involves using a coupling grating to match the wave vectors of the photon and the SPP, which in turn matches their momenta (Taillaert et al., 2006). Finally, small defects in an otherwise planar surface can allow for small

parts of an incident wave to couple with surface plasmons to form SPPs. (Cai et al., 2017; Raether, 1988).

Material Parameters

Three important material parameters in the field of plasmonic metamaterials are electric permittivity ε (epsilon), magnetic permeability μ (mu), and conductivity σ (sigma). The permittivity of a substance denotes the capacitance it demonstrates in the presence of an electric field, the permeability measures the degree to which a substance is magnetized in the presence of a magnetic field, and the conductivity is the relative ability of a substance to conduct electric current. Additionally, permittivity is the function that determines the relationship between the displacement field $\boldsymbol{D}$ and the electric field $\boldsymbol{E}$, while permeability relates the magnetic flux density $\boldsymbol{B}$ to the magnetic field $\boldsymbol{H}$.

The permittivity, permeability, and conductivity can all be expressed as complex numbers, but the definition of complex permittivity has the most relevance to the field of PMMs. Complex permittivity is usually written as a function of the angular frequency of the electric field, ω, like so:

$$\varepsilon_0\varepsilon_r(\omega) = \varepsilon'(\omega) + i\varepsilon''(\omega) = \left|\frac{D_0}{E_0}\right|(\cos(\delta) + i\sin(\delta)) \qquad \text{(Eq. 4)}$$

where ε_0 is the permittivity of free space, ε_r is the relative permittivity of the material, ε' is the real part of the complex permittivity, ε'' is the imaginary part, D_0 and E_0 represent

the magnitudes of the displacement and electric fields respectively, and δ is the loss angle[9], shown in Equation 5. The real part of the permittivity quantifies the stored energy and determines whether the optical response of the material will be capacitive or inductive. Conversely, the imaginary part of the permittivity is related to the conductivity and is therefore tied to the dielectric loss (Parker & Thompson, 2018, pp. 116-117). The loss angle δ is defined by:

$$\delta = \tan^{-1} \frac{\omega\varepsilon'' + \sigma}{\omega\varepsilon'} \quad \text{(Eq. 5)}$$

and represents the phase lag between the electric and magnetic fields in a dielectric material; when the real part is positive, the phase shift is as well, and the material has an intrinsically capacitive response, and when the real part is negative, the material has an inductive response. The ω terms in the equation indicate that the loss angle is frequency dependent.

One of the interesting properties of metamaterials is that the values of many of their physical parameters, like magnetic permeability and electric permittivity, are tunable to specific applications. This tunability leads to the possibility for other properties not found in nature, among them a negative index of refraction.

A plasmonic *material*, in the non-meta sense, is a material for which the real part of the complex permittivity is negative. These are usually gold, silver, or other noble

[9] The loss angle refers to the complex phasor which represents the dielectric losses of a material.

metals, but some other materials exhibit metal-like optical properties in some frequency bands (Boltasseva & Atwater, 2011). In 1968, Russian theoretical physicist Victor Georgievich Veselago published a paper concerning theoretical materials that simultaneously exhibited negative permittivity and negative permeability. (1968). Such materials are also known as negative index or left-handed materials (LHM) referring to the refractive index and the inversion of the right-hand rule[10] used in electromagnetic visualization, respectively.

Normally, if light propagates from one medium into another in ideal circumstances, it will bend (refract) after crossing a boundary called the normal, which is perpendicular to the surface at the point of incidence. In a negative index material, this light would not cross the normal, but would instead be refracted backward (Fig. 5). When a conventional medium has an interface with a negative index medium, Snell's Law of Refraction still applies, regardless of the sign of the variables (Eq. 6). Moreover, the normal components of the wave vectors are parallel at an interface between two conventional media and between two negative index media but are antiparallel at an interface between conventional and negative index media (Caloz & Itoh, 2006, pp. 43-46).

$$\frac{\sin\theta_2}{\sin\theta_1} = \frac{v_2}{v_1} = \frac{n_1}{n_2} \qquad \text{(Eq. 6)}$$

[10] A conventional material, naturally, is known as a right-handed material (RHM).

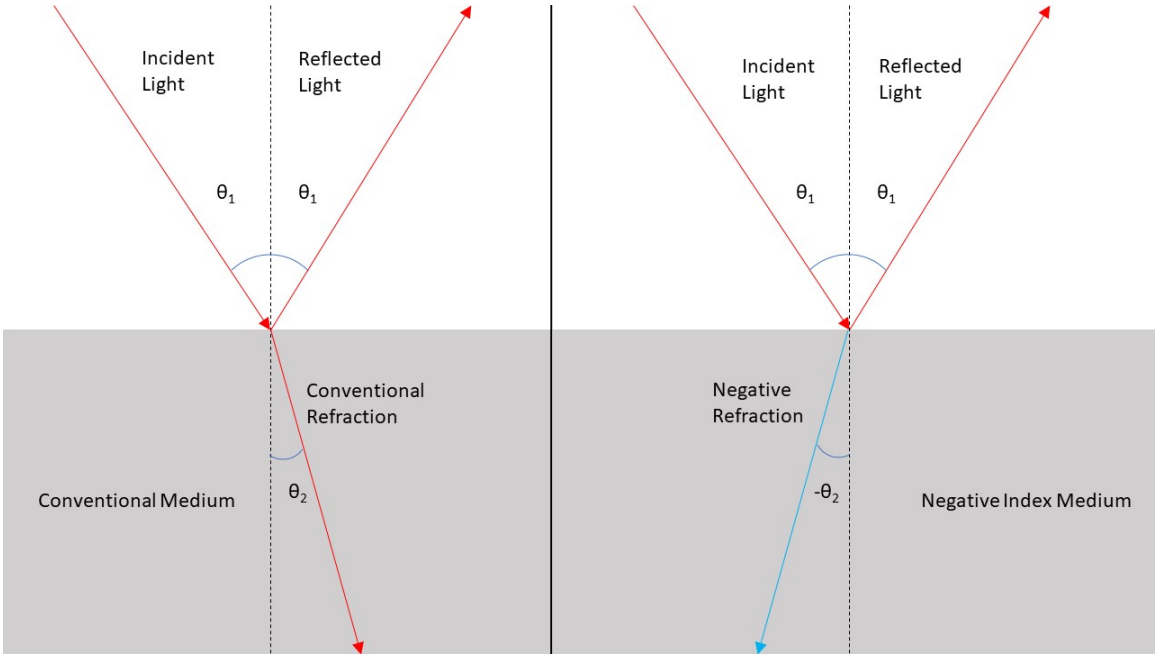

Figure 5: Refraction in conventional and negative index media.

In Equation 6, θ_1 is the angle of incidence, θ_2 is the angle of refraction, v_1 and v_2 are the phase velocities in each medium, and n_1 and n_2 are the indices of refraction for each medium. Since Snell's Law still applies when the refractive index of two media changes sign over their interface, this implies that the group velocity of v_2 is negative when θ_2 is negative. Moreover, the Poynting vector, which represents the directional energy flux of the electromagnetic field (or the direction of a ray of light), will point in the opposite direction of the wave vector, which represents the direction of wave propagation (Fig. 5). The first reported demonstration of negative refraction was accomplished by a collaborative effort between NIST and the California Institute of Technology (Caltech) in 2007, forty years after it was first proposed. The research team

reported that they had achieved two-dimensional narrow-band negative refraction (Lezec, Dionne & Atwater, 2007).

Metamaterial structure. Metamaterials, especially electromagnetic ones, usually consist of a repeating lattice structure made of metallic and dielectric materials on a very small scale. Because of the proximity of the lattice substructures, the properties of the individual substructures of the lattice homogenize, and the metamaterial demonstrates the unique properties for which it was designed.

In plasmonic metamaterials, the substructures are designed such that their features are smaller than the wavelength of incident light and are separated by subwavelength distances. The substructures can take a variety of forms, usually a type of resonator. When light strikes a plasmonic metamaterial, it couples with electrons near the interface and forms surface plasmon polaritons.

Variations on parameters. The possibilities of PMM development are not limited to only two dimensions, nor are they necessarily confined to the visible or infrared sections of the electromagnetic spectrum (although developing PMMs for high-frequency light becomes increasingly difficult due to the surface plasma frequency asymptote described above). The tunability of PMMs to specific applications makes them relevant to almost every field of modern science.

Isotropy. Isotropy, derived from the Greek *isos* (ἴσος, meaning equal) and *tropos* (τρόπος, meaning way) is defined as "exhibiting properties (such as the velocity of light transmission) with the same values when measured along axes in all directions." ("Isotropic", 2019) The opposite of isotropy is anisotropy, which is any restriction on isotropy. Most metamaterials exhibit a high degree of anisotropy with respect to

plasmons, restricting their propagation to a single direction. Isotropic PMMs are currently in development and have several potential applications (Chen et al., 2014).

Optical absorption. Controlling the optical absorption of a system is an important requirement for many applications of PMMs. For applications like enhanced photoemission (Zhukovsky, Babicheva, Uskov, Protsenko, & Lavrinenko, 2013), solar water vaporization and distillation (Neumann et al., 2013), efficient photovoltaic energy production (Clavero, 2014), and thermoelectric magnetic nano-pulses (Tsiatmas et al., 2013), a high absorption rate is advantageous because energy is converted into the desired state more efficiently. Metamaterial absorbers have greater potential for miniaturization, more adaptability, and increased effectiveness relative to their conventional counterparts (Cui et al., 2014).

On the other hand, for information transfer, it is important that absorption and losses be minimized to ensure that the information that is transmitted remains intact. Thermal losses and signal delays are one of the most significant problems preventing fully optically integrated digital circuits (Zia, Schuller, Chandran & Brongersma, 2006; Boltasseva & Atwater, 2011).

Materials used for PMMs. PMMs have been constructed from a variety of materials thus far. The first negative refraction index PMM for visible light was constructed from a silicon sandwich structure, with noble metal films on either side of a silicon wafer. CMOS-compatible PMMs have been constructed from aluminum scandium nitride and titanium nitride, forming a superlattice (multi-material crystal) structure that is thermally stable over a variety of temperatures (Naik et al., 2014). Semi-metals like graphene have a degree of electrical and optical tunability not found in metals (Low &

Avouris, 2014). They are used for several plasmonic applications, like photodetectors for optical communications, (Mueller, Xia & Avouris, 2010), electro-optical broadband modulators for silicon waveguides (Liu et al., 2011), and biosensors (Kabashin, Evans, Pastkovsky, Hendren, & Wurtz, 2009).

Applications

Overview

Plasmonic metamaterials have many applications in many fields of science and technology. They have been used in high-sensitivity biological and chemical sensors, infrared and visible cloaking technology, and nano-scale photovoltaics. Current and upcoming research on PMM applications includes optical computing, nanophotonic data transfer, and microscopy beyond the diffraction limit imposed by the wavelength of visible light.

Biological and Chemical Sensors

Many of the applications of PMMs are related to sensor technology. The high sensitivity of SPPs to heterogeneity in surface thickness or skin depth means that plasmonic sensors can detect nanometer-scale changes in thickness and molecular structure. In a controlled environment, these small changes can provide a method by which to monitor biochemical bonding processes and determine specific factors of the bond structure. Most if not all PMM sensor applications are label-free, meaning they do not use a chemical compound to bind to and label the element.

Brewster Angle Microscopy. In optics, the Brewster angle, or polarization angle, is “an angle of incidence at which there is no reflection of p-polarized light at an uncoated optical surface.” (“Brewster’s Angle,” 2019; Brewster, 1815). A Brewster angle

microscope is a device used to observe the properties of thin films on liquid surfaces, usually a Langmuir-Blodgett film, which consists of one or more monolayer of organic material that is homogeneously adsorbed[11] by immersing a solid substrate into a liquid and transferring the monolayers from the liquid surface to the solid surface. From the observer's perspective, the monolayers are vertically assembled, and the thickness of the film can be accurately determined by adding each monolayer's thickness, due to the homogeneous adsorption of the layers. Brewster angle microscopy can be used to monitor the behavior of the film under different conditions or monitor chemical reactions in the surface.

Plasmonic metamaterials have several applications in this field. First, electromagnetic modulators in the terahertz range must possess high tunability for wave intensity and phase to adequately control such high-frequency signals. Traditional materials do not satisfy these requirements. However, graphene and quartz-based PMMs have been used to construct a new type of modulator, with a tunable Brewster angle, high modulation depth (over 99 percent), and up to 140 degrees of phase tunability (Chen et al., 2018).

Normally, at the Brewster angle, p-polarized light will not exhibit reflection if the medium behind the film is transparent. This suppression of reflection is known as topological darkness. However, if the medium is absorbent, the reflection is not canceled because the medium has a complex index of refraction[12], and the components can no

[11] Meaning that the film layer remains homogeneous relative to other layers during the adsorption process.

[12] The refractive index of a material is a complex number $n = n' + in''$, where the imaginary part n'' represents an attenuation index, also known as a damping constant or extinction coefficient (Shalaev, 2007).

longer cancel out (Coutant et al., 2015). This can be fixed by depositing a plasmonic metamaterial film with a suitable complex refractive index such that the components of the underlying absorbent media are effectively canceled out, restoring the topological darkness condition (Coutant et al., 2015).

Rotational-vibrational spectroscopy. Rotational-vibrational spectroscopy is a subset of molecular spectroscopy focused on the infrared and Raman spectra of gas-phase molecules, and how these relate to the rotational and vibrational energy states of those molecules. The rotational state of a molecule refers to its angular momentum, and the vibrational state refers to a specific mode of the periodic motion of the molecule, known as vibration frequency. Rotational and vibrational states are both quantized, and molecules that undergo rotational or vibrational state changes emit or absorb photons at specific frequencies that can be captured using a spectrometer. Analyzing the frequency allows observers to determine the rotational and vibrational energy states of the molecule.

Infrared range vibrational spectroscopy techniques like surface-enhanced Raman scattering (SERS) and surface-enhanced infrared absorption (SEIRA) were first tested on unaltered, chemically prepared, or roughened metal surfaces, which failed to realize the full potential of the technology due to a comparatively low signal-to-noise ratio (Cheng, Yang & Gao, 2015). Plasmonic metamaterial sensors are a more accurate biochemical sensing method because they can be tuned to generate a stronger response when vibrational mode shifts occur (Cheng, Yang & Gao, 2015).

There are two types of PMM biochemical sensors. The first monitors the collective nanostructure oscillation, while the second observes the resonant behavior of individual meta-molecules. Both methods provide a high degree of sensitivity because the

properties of the PMM can be tuned to resonate at the vibrational modes of specific biomolecules through local near-field enhancement (Cheng, Yang & Gao, 2015). Unfortunately, an air gap of less than 10 nm is often required for optimum PMM sensing, and traditional nanostructure manufacturing processes limit the minimum size of the air gap.

Usually, plasmonic metamaterials are manufactured either by electron beam lithography (EBL) or focused ion beam (FIB) milling. EBL uses a focused beam of electrons to create custom shapes on an electrically sensitive film, and FIB works much the same, except that the beam uses ions instead of electrons. Traditional EBL and FIB milling both suffer from a lack of precision at the scale required (Cheng, Yang & Gao, 2015). A new strategy for increased precision utilizes Fano resonances and electromagnetically induced transparency to increase the precision of the structure and reduce the complexity of the manufacturing process (Cheng, Yang & Gao, 2015). These new metamaterials allowed the researchers to increase the enhance the signal to noise ratio by a factor of 10^5 by tuning the metamaterial's resonant modes to match the vibrational modes of the molecule in question, which has massive implications for the future of biomolecule detection and measurement (Cheng, Yang & Gao, 2015).

Advantages of 3D- vs. 2D-oriented nanostructures. Researchers using 3D-oriented nanostructures for plasmon excitation demonstrated superior performance to normal 2D-oriented structures by bypassing the diffraction limitations of 2D structures. They achieved higher spectral sensitivity and more precise phase response (Aristov, Manousidaki, & Danilov, 2016).

Cloaking Technology

A cloaking device is a device capable of rendering an object invisible to detection in different parts of the electromagnetic spectrum. For decades, cloaking technology has intrigued both science fiction enthusiasts and researchers; in 1966, *Star Trek* writer Paul Schneider wrote the script for an episode titled "Balance of Terror" (McEveety, Schneider, & Roddenberry, 1966). Heavily inspired by submarine warfare movies of the previous decade like *Run Silent, Run Deep* (Wise, Gay, & Beach, 1958) and *The Enemy Below* (Powell, Mayes, & Rayner, 1957), "Balance of Terror" featured a spacecraft that possessed an invisibility cloak, allowing the vessel to disappear and avoid sensor readings, much like the submersion of submarines allowed them to evade detection. Invisibility cloaks have since been included on in other science fiction media such as *Star Wars*, *Stargate* and *Doctor Who.*

In the real world, there are several domains of technology that approach the cloaking devices of science fiction, but the most prominent one uses the tunable properties of metamaterials to manipulate the propagation of incident light, bending or guiding light of certain wavelengths around objects, rendering them invisible in that spectrum. The field within metamaterial research related to this topic is known as transformation optics.

Pendry, Schurig, and Smith (2006) released several papers that described how metamaterials with independent and arbitrary permittivity and permeability values could be used to alter or distort the coordinates by which the field is defined (Figure 6). Such a material would deflect light that would have hit the object, guide the light around it, and return those light rays to the original trajectory, as shown in Figure 7 (2006, p. 1781).

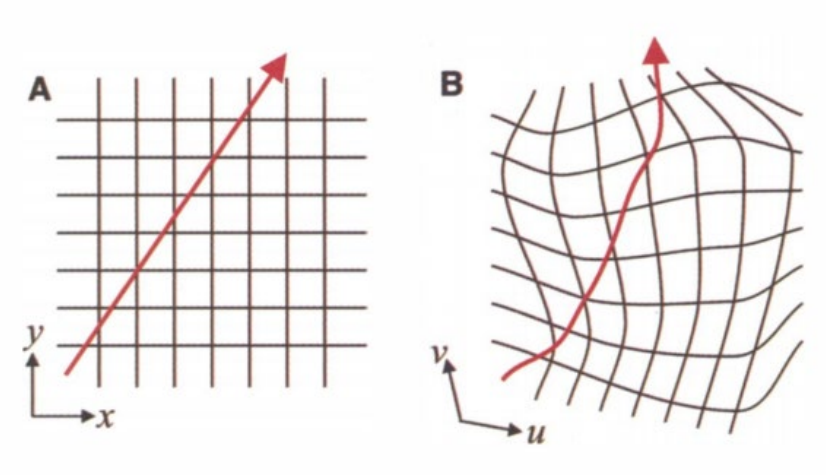

Figure 6: (A) A field line in free space, defined by a rectangular coordinate system with constant permittivity and permeability. (B) The same field line in a non-rectangular coordinate system, caused by independently varying permittivity and permeability. Reprinted from "Controlling Electromagnetic Fields," by J. B. Pendry, D. Schurig and D. R. Smith, 2006, *Science, 312*(5781), p. 1780. Copyright 2006 by the American Association for the Advancement of Science.

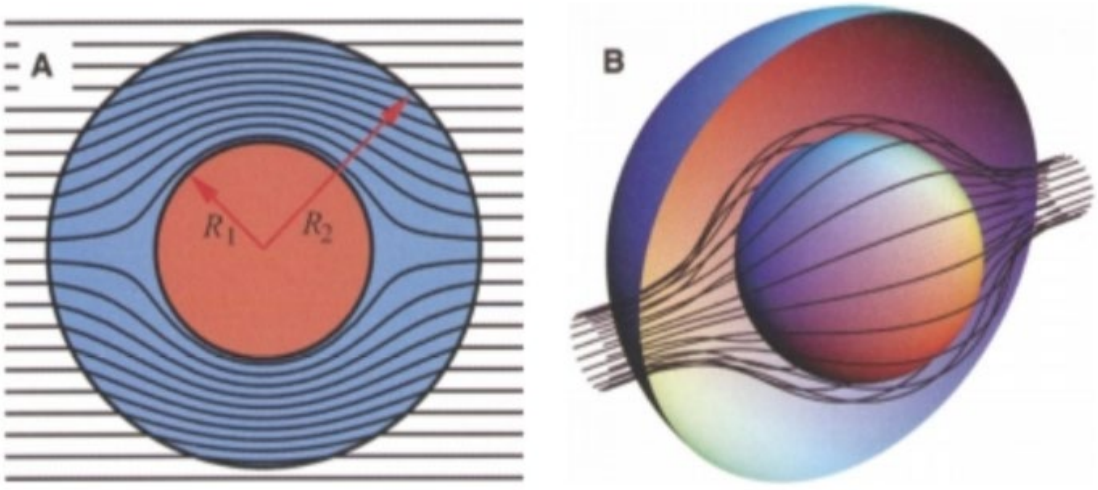

Figure 7: (A) A two-dimensional cross-section of rays striking the cloaking system, diverted and then returned by the cloaking material. (B) A 3D view of the same process. Reprinted from "Controlling Electromagnetic Fields," by J. B. Pendry, D. Schurig and D. R. Smith, 2006, *Science, 312*(5781), p. 1781. Copyright 2006 by the American Association for the Advancement of Science.

This distortion of the coordinates that represent the space around the object can be thought of as compressing or stretching spacetime itself, in the context of the local system (Pendry et al., 2006). Because the radiation is guided around the hidden object and does not interact with it, the cloak would allow for an object with arbitrary properties to be concealed in the device (Pendry et al., 2006). The field line in question can represent either the electric (**D**) or magnetic (**B)** fields, or the Poynting vector **S**. Maxwell's equations do not vary through coordinate transforms, so the field lines' relation to the coordinate system does not change. Rather, the coordinate system becomes nonrectangular, and the field line's representation in that coordinate system changes accordingly.

For light rays that would normally be directed toward the center of the object, the direction in which they must be redirected becomes increasingly arbitrary, and the renormalized values of permittivity and permeability must change very rapidly. Additionally, the anisotropy of the medium must conform to the degree that the encompassing space has been compressed anisotropically (Figure 6), to ensure that rays are redirected properly. Pendry et al. pointed out that these would be some of the most challenging issues to overcome before cloaking technology could become reality (2006).

Since Pendry et al. (2006) released their initial research on the subject, numerous prototypes have been released that demonstrate the properties they described. The first realization of their theory came about only months after its publication, when Schurig et al. created a narrow band microwave cloak for a copper cylinder (2006), inspiring the work of many subsequent researchers. For example, researchers at Yonsei University in Seoul created a working prototype of a "smart" metamaterial, which could not only

perform a coordinate transform, but also "acquires its properties automatically from its own elastic deformation" in the microwave range (Shin et al., 2012).

Several theories for plasmonic cloaking in the visible light range were discussed after the initial cloaking theory, including alternating plasmonic and non-plasmonic cylindrical layering (Bilotti, Tricarico, & Vegni, 2010), 3D homogeneous polyhedral transformation (Zheng et al., 2018), and symmetrical satellite cloaking (Silveirinha, Alù, & Engheta, 2008), among others (Fleury & Alu, 2014). Cloaking has since been achieved in the near-infrared spectrum (Gabrielli, Cardenas, Poitras & Lipson, 2009), but at the time of this writing, no strictly metamaterial-based prototype of a visible light cloak has yet been demonstrated. This is primarily due to the plasmon curve approaching the surface plasma frequency asymptote in Figure 3. However, visible range cloaking has been proven using another technique called carpet cloaking, in which a flexible object with the appearance of a mirror is laid over an object, such that the deformation caused by the concealed object is not detectable (Gladden et al., 2011).

Quantum invisibility. Researchers have probed the question of how to shield an object from certain quantum properties of nearby particles. Lee & Lee at the National Tsing-Hua University in Taiwan developed a theoretical model for core-shell nanoparticles that stretch spacetime around themselves such that the probability of an object existing inside the nanoparticles is effectively zero (2014). This approach is like those used for optical cloaking, but it bases its precepts on Schrodinger's equation, which governs the probability of particles occupying a region of space, rather than Maxwell's equations, which describe how electromagnetic fields are generated and changed by the presence and movement of charges. Such a device could be used to shield sensitive nano-

structures from interference or damage from nearby electrons, without disturbing the environmental quantum probability (Lee & Lee, 2014).

Photovoltaics

Photovoltaics is a science and engineering field concerned with the conversion of light to electricity. It is one of the most well-known and widely utilized renewable energy fields. The cost of solar power continues to decrease, to the point where solar energy now costs the same or less to implement than implementing new fossil fuel solutions (Griffin, 2017).

Plasmonic structures for thin-film cells. Most solar cells in the current market are silicon wafers a few hundred micro-meters thick that use a pyramidal surface to scatter light into the cell, where the photon's momentum will collide with electrons at the base of the cell, initiating current flow (Atwater & Polman, 2010). Because of the high cost of manufacturing and acquiring high quality silicon, thin-film solar cells, on the scale of 1-2 μm, are very attractive as power generation alternatives (Atwater & Polman, 2010). Thin-film cells have several advantages over normal cells: in addition to using much less material, they can be deposited on cheap substrates like glass and plastic, and they can effectively use rarer semiconductor materials like indium and tellurium (Atwater & Polman, 2010). Unfortunately, thin-film cells have a low absorbance rate, so developing structures that can trap light near the cell is the focus of much research in photovoltaics (Atwater & Polman, 2010).

Atwater and Polman (2010) suggest three geometric methods by which plasmonic structures can increase photocurrent in thin-film cells, seen in Figure 8. The first uses metallic nanoparticles as scattering elements and traps light waves between the substrate

Figure 8: (a) Nanoparticles used as a scattering and trapping medium. (b) Nanoparticles used as subwavelength antennas to excite LSPs. (c) Corrugated metal surface traps light and excites surface plasmons. Reprinted from "Plasmonics for improved photovoltaic devices," by H. A. Atwater and A. Polman, 2010, *Nature Materials, 9*(3), pp. 205-213. Copyright 2010 by the Nature Publishing Group.

and a thin absorbent layer, the second method uses nanoparticles as sub-wavelength antennas, exciting localized surface plasmons (LSPs) that induce a current, and the third uses a corrugated metal surface to create and sustain surface plasmons, the motion of which induces current. According to Atwater & Polman, using these methods may allow photovoltaic cells to be shrunk by a factor of 10 to 100 (2010).

Optical Computing and Nanophotonic Circuits

Optical computing uses photons from lasers or diodes as a data transmission medium for computation. Some research in this area is devoted to creating optical components that are compatible with current electronic computers; however, about 30% of energy is lost when electrical energy is converted to light, and vice versa (Nolte, 2001, p. 34), creating the need for repeaters (Zia, Schuller, Chandran & Brongersma, 2006). There is also a size mismatch between electronic and dielectric photonic components, creating an obstacle to scalability (Zia, Schuller, Chandran & Brongersma, 2006). Finally, interconnecting photonic and electrical components causes significant delay

times, especially at higher clock frequencies (Zia, Schuller, Chandran & Brongersma, 2006).

A more viable long-term solution is the development of all-optical computers, such that electrons are not utilized (Nolte, pp. 34-35), but this will take significant time and investment to implement. Computers that use partial or fully integrated optical components have several advantages over electronic computers.

Advantages of optical computing. Electronic data transfer through wires and components dissipates heat. Photons, on the other hand, do not exhibit resistive loss, and overall energy loss is much smaller (Brongersma & Shalaev, 2010). Also, photonic circuitry allows for multiple signals to be sent down the same transmission line at once via frequency multiplexing.

The current minimum size for an electron-based transistor is around 10 nm. This is because transistors below this size allow electrons to quantum tunnel past them (Kumar, 2015). Additionally, the smaller electronic components become, the more noticeable the effects of inductive and capacitive propagation delay (Ismail & Friedman, 2000). Photons do not quantum tunnel and are not affected by capacitance and inductance.

Critics of optical computing point out that many of the proposed solutions for optical digital processing are highly speculative (Tucker, 2010). Tucker describes several key points on which a more realistic perspective should be applied before claiming that optical computing is a perfect solution, the most important of which are listed below.

First, nonlinear optical elements don’t currently possess some of the functions required to be competitive with electronic circuits. Secondly, many proponents of optical

computing claim that passive optical elements are lossless, which is not strictly true. Losses still exist in optical circuits, especially with many components. Third, optical memory systems need significant development before reaching the performance and cost efficiency of electronic memory. Finally, the cost of optical components would need to overcome the vast economies of scale that drive the global electronics industry to be competitive (Tucker, 2010).

Plasmonic applications. Plasmonic metamaterials can be used to offset some of the energy loss from electron-photon conversion between dielectric photonic components and electronic ones (Zia, Schuller, Chandran & Brongersma). Very recent research has also suggested that PMMs may play a very important role in developing fully photonic computers, specifically in the design of optical switches, optical oscillators, and optical traps (Rashed, Mohammed, Zaky, Amiri & Yupapin, 2019).

Superlenses and Subwavelength Microscopy

In 1873, Ernst Abbe formulated a fundamental minimum limit for the resolution of an optical system. According to Abbe's derivations, light of wavelength λ traveling in a medium with a refractive index of n will have a minimum resolvable distance d of:

$$d = \frac{\lambda}{2n \sin\theta} = \frac{\lambda}{2NA} \qquad \text{(Eq. 5)}$$

where the n sin (θ) term is called the numerical aperture, with a range of 1.4-1.6. The minimum resolution limit using conventional materials is approximately:

$$d \simeq \frac{\lambda}{3} \quad \text{(Eq. 6)}$$

For scale, green light in the visible range has a wavelength of around 500 nm, so if we assume the numerical aperture to be approximately one, this gives us a minimum resolution of 250 nm. This allows to observation of most biological cells (which on average are about 25 μm), but not viruses (100 nm), proteins (5 nm), or smaller molecules (>1 nm). The visualization of small structures and organisms like these is vital to continued research in biology, chemistry, materials science, and other fields.

One of the most interesting applications of plasmonic metamaterials is the development of superlenses; lenses that can transcend the diffraction limit of conventional materials to resolve very small objects. In 2000, Pendry was the first to suggest that such a lens might be possible using negative refractive index materials like Veselago (1968) had suggested years before (Pendry, 2000). The first superlens to surpass the diffraction limit used a negative-index metamaterial in the microwave range and provided resolution three times better than the diffraction limit (Grbic & Eleftheriades, 2004). Since then, PMMs have been used for superlens electromagnetic wave imaging (Aydin & Ozbay, 2007), Luneberg and Eaton lenses (Zentgraf, Liu,

Mikkelsen, Valentine & Zhang, 2011), and superlenses with more than a decade of bandwidth (Kundtz & Smith, 2009).

Conclusion

Plasmonic metamaterials are the result of centuries of human achievement, and collaboration between many diverse fields of science and engineering. They have enabled advances in medicine, computation, stealth technology, and solar power generation, and they force the scientific community to continually question their preconceptions about what is possible. As research in this fascinating field continues, even more frontiers will open for the multidisciplinary field of plasmonic metamaterials.

References

Abbe, E. (1873). Beiträge zur Theorie des Mikroskops und der mikroskopischen Wahrnehmung [Contributions to the theory of the microscope and the microscopic perception]. *M. Schulze's Archive für Mikroskopische Anatomie 9*, 413. doi:10.1007/BF02956173

Aristov, A. I., Manousidaki, M., & Danilov, A. (2016). 3D plasmonic crystal metamaterials for ultra-sensitive biosensing. *Scientific Reports, 6*, 25380. doi:10.1038/srep25380

Ashby, M. F., Ferreira, Paulo J. S. G, & Schodek, D. L. (2009). *Nanomaterials, nanotechnologies and design: An introduction for engineers and architects*. Oxford: Butterworth-Heinemann

Atwater, H. A., & Polman, A. (2010). Plasmonics for improved photovoltaic devices. *Nature Materials, 9*(3), 205-213. doi:10.1038/nmat2629

Aust, E. F., Sawodny, M., Ito, S., & Knoll, W. (1994). Surface plasmon and guided optical wave microscopies. *Scanning, 16*(3), 353-362. doi:10.1002/sca.4950160312

Aydin, K., & Ozbay, E. (2007). Left-handed metamaterial based superlens for subwavelength imaging of electromagnetic waves. *Applied Physics A, 87*(2), 137-141. doi:10.1007/s00339-006-3817-4

Barger, V., Marfatia, D., & Whisnant, K. (2012). Model building. In *The physics of neutrinos* (pp. 99-115). Princeton, NJ: Princeton University Press. Retrieved from http://www.jstor.org/stable/j.cttq94kv.12

Bilotti, F., Tricarico, S., & Vegni, L. (2010). Plasmonic metamaterial cloaking at optical frequencies. *IEEE Transactions on Nanotechnology, 9*(1), 55-61. doi:10.1109/tnano.2009.2025945

Boltasseva, A., & Atwater, H. A. (2011). Low-loss plasmonic metamaterials. *Science, 331*(6015), 290-291. doi:10.1126/science.1198258

Brewster, D. (1815). On the laws which regulate the polarisation of light by reflexion from transparent bodies. *Philosophical Transactions of the Royal Society of London, 105*, 125-159. Retrieved from http://www.jstor.org/stable/107362

Brewster's Angle. (n.d.). In *RP Photonics Encyclopedia*. Retrieved April 1, 2019, from https://www.rp-photonics.com/brewsters_angle.html

Brongersma, M., & Shalaev, V. (2010). The case for plasmonics. *Science, 328*(5977), new series, 440-441. Retrieved from http://www.jstor.org/stable/40655768

Cai, T., Dutta, S., Aghaeimeibodi, S., Yang, Z., Nah, S., Fourkas, J. T., & Waks, E. (2017). Coupling emission from single localized defects in two-dimensional semiconductor to surface plasmon polaritons. *Nano Letters, 17*(11), 6564-6568. doi:10.1021/acs.nanolett.7b02222

Caloz, C., & Itoh, T. (2006). *Electromagnetic metamaterials: Transmission line theory and microwave applications: The engineering approach*. Hoboken, NJ: John Wiley & Sons.

Carroll, S. (2007). *Dark matter, dark energy: The dark side of the universe.* Chantilly, VA: The Great Courses.

Carroll, S. (2013, January 8). Bosons. *Symmetry*. Retrieved March 16, 2018, from https://www.symmetrymagazine.org/article/january-2013/bosons

Chen, Z., Chen, X., Tao, L., Chen, K., Long, M., Liu, X., . . . Xu, J. (2018). Graphene controlled Brewster angle device for ultra broadband terahertz modulation. *Nature Communications, 9*(1). doi:10.1038/s41467-018-07367-8

Chen, C., Ishikawa, A., Tang, Y., Shiao, M., Tsai, D. P., & Tanaka, T. (2014). Uniaxial-isotropic metamaterials by three-dimensional split-ring resonators. *Advanced Optical Materials, 3*(1), 44-48. doi:10.1002/adom.201400316

Cheng, F., Yang, X., & Gao, J. (2015). Ultrasensitive detection and characterization of molecules with infrared plasmonic metamaterials. *Scientific Reports, 5*(1). doi:10.1038/srep14327

Clavero, C. (2014). Plasmon-induced hot-electron generation at nanoparticle/metal-oxide interfaces for photovoltaic and photocatalytic devices. *Nature Photonics*, *8*(2), 95.

Coutant, C., Ravaine, S., Wang, X., Toudert, J., Ponsinet, V., & Barois, P. (2015). Plasmonic metamaterials for ultra-sensitive sensing: Topological darkness. *Rendiconti Lincei, 26*(S2), 175-182. doi:10.1007/s12210-015-0404-7

Cui, Y., He, Y., Jin, Y., Ding, F., Yang, L., Ye, Y., . . . He, S. (2014). Plasmonic and metamaterial structures as electromagnetic absorbers. *Laser & Photonics Reviews, 8*(4), 495-520. doi:10.1002/lpor.201400026

Dragoman, M., & Dragoman, D. (2009). *Nanoelectronics: Principles and devices* (Second ed.). Boston: Artech House.

Fleury, R., & Alu, A. (2014). Cloaking and invisibility: A review. *Progress in Electromagnetics Research*, *147*, 171-202. doi:10.1103/PhysRevB.78.205109

Gabrielli, L. H., Cardenas, J., Poitras, C. B., & Lipson, M. (2009). Silicon nanostructure cloak operating at optical frequencies. *Nature Photonics, 3*(8), 461-463. doi:10.1038/nphoton.2009.117

Gladden, C., Gharghi, M., Zentgraf, T., Liu, Y., Yin, X., Valentine, J., & Zhang, X. (2011). A carpet cloak device for visible light. *Nano Letters, 11*(7), 2825-2828. doi:10.1364/fio.2011.fmi2

Grbic, A., & Eleftheriades, G. V. (2004). Overcoming the diffraction limit with a planar left-handed transmission-line lens. *Physical Review Letters,92*(11). doi:10.1103/physrevlett.92.117403

Griffin, A. (2017, January 04). Solar and wind power cheaper than fossil fuels for the first time. *The Independent*. Retrieved April 3, 2019, from https://www.independent.co.uk/environment/solar-and-wind-power-cheaper-than-fossil-fuels-for-the-first-time-a7509251.html

Hornyak, G. L., Dutta, J., Tibbals, H. F., & Rao, A. K. (2008). *Introduction to nanoscience*. Boca Raton: CRC Press.

Ismail, Y. I., & Friedman, E. G. (2000). Effects of inductance on the propagation delay and repeater insertion in VLSI circuits. *IEEE Transactions on Very Large Scale Integration (VLSI) Systems, 8*(2), 195-206. doi:10.1109/92.831439

Kabashin, A. V., Evans, P., Pastkovsky, S., Hendren, W., & Wurtz, G. (2009). Plasmonic nanorod metamaterials for biosensing. *Nature Materials, 8*(11), 867-871. doi:10.1038/nmat2546

Kretschmann, E., & Raether, H. (1968). Notizen: Radiative decay of non-radiative surface plasmons excited by light. *Zeitschrift Für Naturforschung A*, *23*(12), 2135-2136. doi:10.1515/zna-1968-1247

Kumar, S. (2015). Fundamental limits to Moore's law. arXiv:1511.05956

Kundtz, N., & Smith, D. R. (2010). Extreme-angle broadband metamaterial lens. *Nature Materials 9*(2), 129-132. doi:10.1038/nmat2610

Lee, J. Y., & Lee, R. (2014). Hiding the interior region of core-shell nanoparticles with quantum invisible cloaks. *Physical Review B, 89*(15). doi:10.1103/physrevb.89.155425

Lezec, H. J., Dionne, J. A., & Atwater, H. A. (2007). Negative refraction at visible frequencies. *Science, 316*(5823), 430-432. doi:10.1126/science.1139266

Liu, M., Yin, X., Ulin-Avila, E., Geng, B., Zentgraf, T., Ju, L., . . . Zhang, X. (2011). A graphene-based broadband optical modulator. *Nature, 474*, 64-67. doi:10.1038/nature10067

McEveety, V. (Director), & Schneider, P., & Roddenberry, G. (Writers). (1966, December 15). Balance of terror [Television series episode]. In *Star Trek*. New York, New York: NBC.

Naik, G. V., Saha, B., Liu, J., Saber, S. M., Stach, E. A., Irudayaraj, J. M., . . . Boltasseva, A. (2014). Epitaxial superlattices with titanium nitride as a plasmonic component for optical hyperbolic metamaterials. *Proceedings of the National Academy of Sciences, 111*(21), 7546-7551. doi:10.1073/pnas.1319446111

Neumann, O., Urban, A. S., Day, J., Lal, S., Nordlander, P., & Halas, N. J. (2012). Solar vapor generation enabled by nanoparticles. *ACS nano*, *7*(1), 42-49.

Nolte, D.D. (2001). *Mind at light speed: a new kind of intelligence*. New York, New York: Simon and Schuster.

Otto, A. (1968). Excitation of nonradiative surface plasma waves in silver by the method of frustrated total reflection. *Zeitschrift Für Physik A Hadrons and Nuclei, 216*(4), 398-410. doi:10.1007/bf01391532

Parker, M., Thompson, B. (2005). *Physics of optoelectronics*. Boca Raton: CRC Press. doi:10.1201/9781420027716

Pendry, J. B. (2000). Negative refraction makes a perfect lens. *Physical Review Letters, 85*(3966). doi:10.1103/PhysRevLett.85.3966

Pendry, J. B., Schurig, D., & Smith, D. (2006). Controlling electromagnetic fields. *Science, 312*(5781), 1780-1782. doi:10.1126/science.1125907

Powell, D. (Director), & Mayes, W., & Rayner, D. A. (Writers). (1957). *The enemy below* [Motion picture on DVD]. United States: Twentieth Century Fox.

Raether, H. (1988). *Surface plasmons on smooth and rough surfaces and on gratings*. Berlin: Springer-Verlag.

Rashed, A. N., Mohammed, A. E., Zaky, W. F., Amiri, I., & Yupapin, P. (2019). The switching of optoelectronics to full optical computing operations based on nonlinear metamaterials. *Results in Physics,13*, 102152. doi:10.1016/j.rinp.2019.02.088

Regal, C. A., Greiner, M., & Jin, D. S. (2004). Observation of resonance condensation of fermionic atom pairs. *Physical Review Letters, 92*(4). doi:10.1103/physrevlett.92.040403

Shin, D., Urzhumov, Y., Jung, Y., Kang, G., Baek, S., Choi, M., . . . Smith, D. R. (2012). Broadband electromagnetic cloaking with smart metamaterials. *Nature Communications, 3*, 1213. doi:10.1038/ncomms2219

Taillaert, D., Laere, F. V., Ayre, M., Bogaerts, W., Thourhout, D. V., Bienstman, P., & Baets, R. (2006). Grating couplers for coupling between optical fibers and nanophotonic waveguides. *Japanese Journal of Applied Physics*, *45*(8A), 6071-6077. doi:10.1143/jjap.45.6071

Tsiatmas, A., Atmatzakis, E., Papasimakis, N., Fedotov, V., Luk'yanchuk, B., Zheludev, N. I., & de Abajo, F. J. G. (2013). Optical generation of intense ultrashort magnetic pulses at the nanoscale. *New Journal of Physics*, *15*(11), 113035.

Veselago, V. G. (1968). The electrodynamics of substances with simultaneously negative values of ε and μ. *Soviet Physics Uspekhi*, *10*(4), 509-514. doi:10.1070/pu1968v010n04abeh003699

Wise, R. (Director), & Gay, J., & Beach, E. L. (Writers). (1958). *Run silent, run deep* [Motion picture on DVD]. United States: UA/Hecht-Hill-Lancaster.

Zia, R., Schuller, J. A., Chandran, A., & Brongersma, M. L. (2006) Plasmonics: the next chip scale technology. *Materials Today, 9*(7-8), 20-27. doi:10.1016/S1369-7021(06)71572-3

Zentgraf, T., Liu, Y., Mikkelsen, M. H., Valentine, J. & Zhang, X. (2011) Plasmonic Luneberg and Eaton lenses. *Nature Nanotechnology*, *6*(3), 151-155. doi:10.1038/nnano.2010.282

Zheng, B., Zhu, R., Jing, L., Yang, Y., Shen, L., Wang, H., . . . Chen, H. (2018). 3D Visible-light invisibility cloak. *Advanced Science, 5*(6). doi:10.1002/advs.201800056

Zhukovsky, S. V., Babicheva, V. E., Uskov, A. V., Protsenko, I. E., & Lavrinenko, A. V. (2014). Enhanced electron photoemission by collective lattice resonances in plasmonic nanoparticle-array photodetectors and solar cells. *Plasmonics*, *9*(2), 283-289.